

Reversible Synthesis of Structured MOF-to-Metal Oxide Nanorods

Jayraj N. Joshi ^a, Colton M. Moran ^a, Harold P. Feininger^a, Krista S. Walton ^{a*}

^aSchool of Chemical and Biomolecular Engineering
Georgia Institute of Technology
311 Ferst Drive NW
Atlanta, Georgia 30332 USA
E-mail: krista.walton@chbe.gatech.edu

Supplemental Information

Table of Contents

Experimental Methods: Synthesis and Materials Preparation	1-2
Experimental Methods: Characterization Techniques	2-3
Supporting Figures and Tables	4-7
Supplementary Information References	8

Experimental Methods

Synthesis and Materials Preparation

MIL-53(Al) produced from insoluble aluminum materials was used to create derived oxide/carbon composites in this study. MOF production procedures are available in our previous report.¹ Specifically, Al₄C₃-derived MIL-53(Al) and MIL-53(Al) grown from aluminum alloy mesh (mesh purchased from TWP Inc) was utilized to create *MIL-53(Al)-oxide* materials discussed here. Both MOFs and MOF-derived composites were degassed under vacuum at 150°C for 24h before all analyses and synthesis procedures. All other reagents were acquired commercially without further purification.

MIL-53(Al)-oxide: 300 mg of Al₄C₃-derived MIL-53(Al) was loaded onto a silica boat. The boat was then placed in a 20" long, 1" O.D. quartz tube. The assembly was inserted into a horizontal tube furnace, described previously by Moran et al.² The tube was evacuated with argon (Airgas 99.999%) at a flow rate of 150 mL min⁻¹ for at least 30 minutes to purge out air trapped in the tube. Then, the sample was heated to 600°C with a ramp rate of 5°C/min. MIL-53(Al) was allowed to pyrolyze isothermally at 600°C for 8h, and then cooled naturally. After cooling, the assembly was deconstructed, and the newly-synthesized *MIL-53(Al)-oxide* powder was collected. Yields were assessed by weighing the loaded silica boat before and after pyrolysis to quantify mass loss.

Iron oxide-impregnated MIL-53(Al)-oxide: Impregnated materials were made via the incipient wetness method. First, 300 mg of Al₄C₃-derived MIL-53(Al) was degassed and placed in a 20mL scintillation vial. Simultaneously, 7.86g of 99% pure iron (III) nitrate nonahydrate, purchased from Acros, was mixed into 10mL of DI water in a 20mL scintillation vial with magnetic stirring. The mixture was agitated at room temperature until the solute completely dissolved. Based on the estimated pore volume of Al₄C₃-derived MIL-53(Al) (~0.28 cc g⁻¹), 3.5x the volume of the available pore volume of the MOF (84μL × 3 = 294μL) was assumed to supersaturate the pore space. Accordingly, 294μL of the iron nitrate solution was dispensed onto the MOF through 5 additions (59μL each) using a micropipetter. Between each addition, the powder slurry was quickly mixed with a dry glass rod while sonicating the entire vial to promote impregnate integration. After impregnation of the salt was completed, the powder was allowed to dry briefly, and was then added to a silica boat for pyrolysis. MOF pyrolysis thereafter was carried out in the same manner as described above.

MIL-53(Al) regrowth cycles: MIL-53(Al) growth cycles from *MIL-53(Al)-oxide* were carried out by repeating two general steps-

- (1) Pyrolysis of Al_4C_3 -derived MIL-53(Al)
- (2) Solvothermal growth of MIL-53(Al) from *MIL-53(Al)-oxide*

Step (2) was achieved using the same general procedure described for Al_4C_3 -derived MIL-53(Al) growth reported previously, but instead assumes the metal precursor has a stoichiometry of Al_2O_3 .¹ As an example, for Cycle 1 36.9 mg of *MIL-53(Al)-oxide* was placed in a stainless steel-lined 20mL PTFE reactor with 361.1mg of terephthalic acid (98% from Sigma Aldrich) and 3.9 mL DMF ($\geq 98.9\%$ from Sigma Aldrich). The reactor was then sealed and heated isothermally at 220°C for 24h. After cooling, the mixture was filtered by gravity, and washed with N,N-dimethylformamide and then methanol three time each. The filtered Cycle 1 MOF was then allowed to dry in a chemical hood overnight. Finally, the powder was collected and stored in a cool, dry location.

Characterization Techniques

N₂ Physisorption Analysis: A Quantachrome Quadrasorb SI volumetric system with 5.11 QuadraWin™ software package was used to collect nitrogen adsorption data at 77K. Sample quantities between 50-100mg (after degassing) were utilized in measurements. BET surface area measurements were approximated using a pressure range of $P/P_0 = 0.005-0.03$.³ Total pore volumes are reported at $P/P_0 = 0.8$ to avoid over-approximation from N_2 condensation at high pressures at 77K.

Quenched Solid Density Functional Theory (QSDFT) was utilized through QuadraWin™ to create pore size distributions for MOF-derived oxide-based composites. To account for the surface heterogeneity and multimodal pore systems apparent in *MIL-53(Al)-oxide*, an adsorption branch slit/cylindrical pore model was assumed using a N_2 adsorbate and carbon adsorbent.

Powder X-ray Diffraction (PXRD): PXRD data was acquired using an X'Pert X-ray PANalytical diffractometer. $\text{Cu K}\alpha$ radiation ($\lambda = 1.5418 \text{ \AA}$) was sourced to produce X-rays. Powder samples were first gently ground and packed tightly onto low-intensity background holders. These holders were then rotated during data collection. Scans were carried out at room temperature with a range of $2\theta = 4^\circ - 60^\circ$ and step size of 0.02° .

Scanning Electron Microscopy (SEM)/Energy Dispersive Spectroscopy (EDS): A Zeiss Ultra 60 Field Emission (FE) SEM was used to acquire electron images. Samples were placed onto carbon tape secured on image stands prior to imaging. Accelerating voltage as low as 1keV was used to image nanorod surface texture features depicted in this report for *MIL-53(Al)-oxide*, and a range of voltages from 1-20keV was used to image materials.

EDS measurements were attained using the same apparatus. An accelerating voltage of at least 10keV was utilized while collecting EDS data. AZtec software was used to process EDS data, quantify compositions, and create elemental mapping reports.

Inductively Coupled Plasma Optical Emission Spectroscopy (ICP-OES): Aluminum, iron, and sulfur mass fractions were determined in part through ICP-OES measurements. About 75 mg of tested sample batches were divided into three portions (25 mg each) to provide repeat measurements on each batch. Powder samples were then dissolved through high temperature alkali fusion with sodium carbonate, as opposed to typical acid digestion with nitric acid to prevent possible loss of sulfur. After fusion, the material was dissolved in a 6N hydrochloric acid solution. Dissolved aliquots were then analyzed with a Perkin Elmer Optima 3000 DV ICP Emission Spectrometer.

Acquired sulfur loadings are assumed to be stoichiometrically related to hydrogen sulfide degradation through a 1:1 molar ratio.

X-ray Photoelectron Spectroscopy (XPS): A Thermo K-alpha was used to collect XPS measurements. The instrument utilizes a monochromated Al K α source, with a double-focusing hemispherical analyzer. High resolution spectra were acquired and presented here for sulfur and iron. Measurement parameters include 50 ms dwell time, 50 eV pass energy, a 0.1eV step size, and 400 μ m diameter spot size.

Humid Hydrogen Sulfide Adsorption Experiments

A previously described fixed-bed gas adsorption apparatus was utilized to conduct humid H₂S removal experiments in this work.⁴ Humid H₂S streams were created by mixing the following streams, where both gas mixtures were sourced from cylinders purchased from Airgas without further purification:

1. Dry hydrogen sulfide (~4988ppm) with balance nitrogen
2. Ultra Zero grade air
 - a. Dry air was passed through a sealed stainless steel vessel containing DI water.

Approximately 150-200mg of samples were first placed in a fritted thermal desorption tube. Simultaneously, stream (2) was allowed to equilibrate through a separate purge line for about 90min, reaching a relative humidity of ~85%. Samples were pre-conditioned under flow of the humidified air stream at 50mL min⁻¹ for 1h, while heating to 200°C using insulated heat tape. The sample was then allowed to cool to 20°C.

To start the experiment, stream (1) was mixed with (2). The streams were mixed in a 4:1 volumetric ratio of acid gas-to-humidified air— 40mL min⁻¹ (1) and 10mL min⁻¹ (2). Upon mixing, the streams were then sent to the sample bed. Exposure tests at 20°C were terminated after 3h, and samples were flushed with dry air for 30min afterwards to purge out residual H₂S. Powder samples were then collected and degassed at 200°C under vacuum prior to other measurements described in this work.

Supporting Figures and Tables

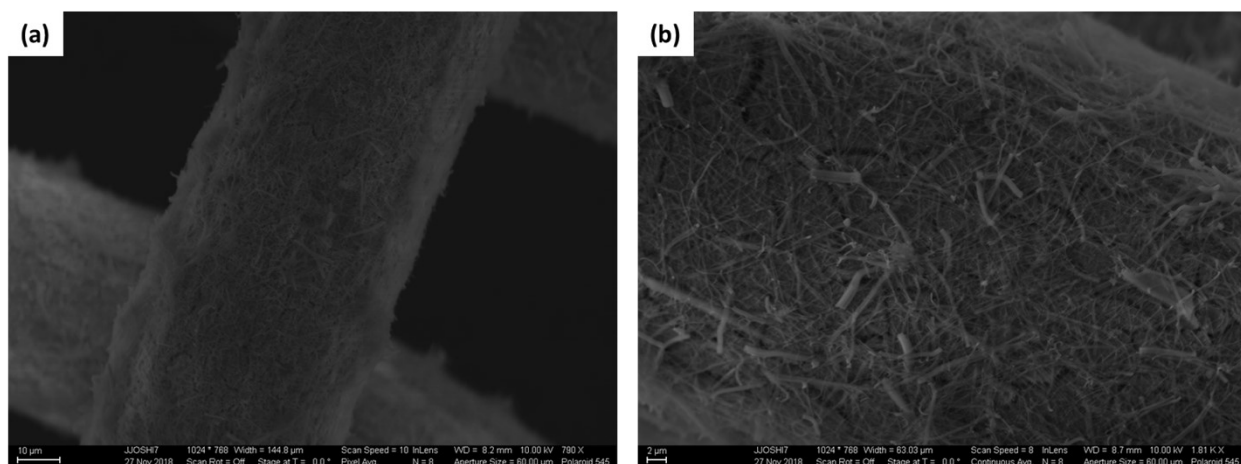


Figure S1. Pyrolyzed MIL-53(Al) derived from aluminum mesh at (a) 790X and (b) 1810X magnification

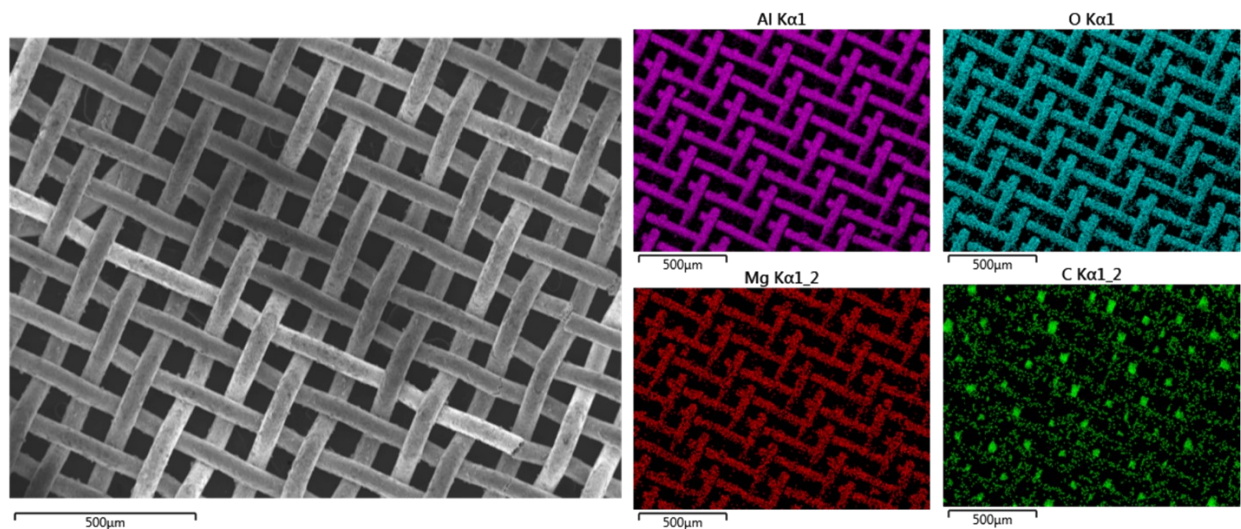


Figure S2. Elemental mapping of aluminum mesh-derived MIL-53(Al) after pyrolysis. C Kα data confirm residual carbon from pyrolyzed linker remains on surface. The mesh is an alloy between aluminum and magnesium, leading to Mg detection.

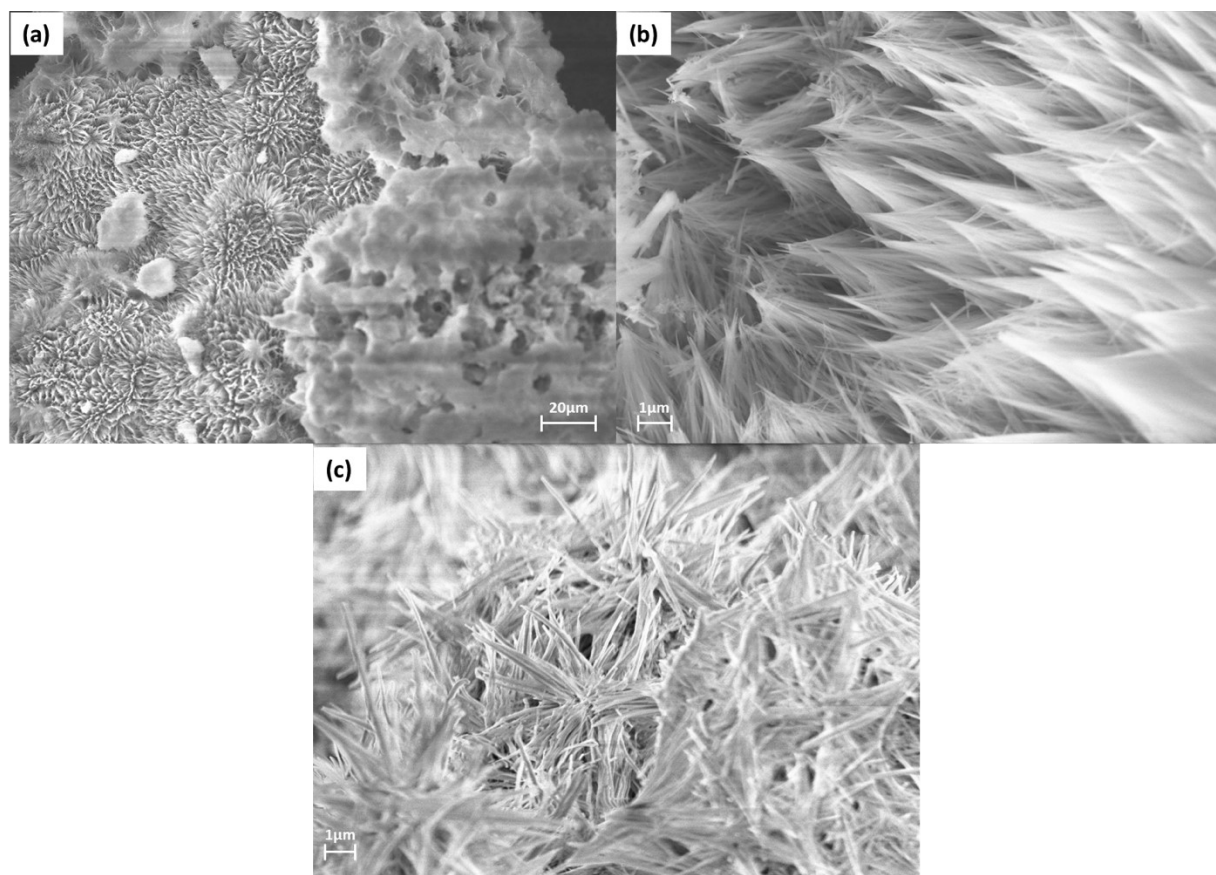


Figure S3. Images of regrown MIL-53(Al) from *MIL-53(Al)-oxide* in (a-b) one and (c) two growth cycles

Table S1. Porosity data from MIL-53(Al) growth cycles

MIL-53(Al)	BET Surface Area (m ² g ⁻¹)	^a Total Pore Volume (cc g ⁻¹)
^b Parent MOF	1154.2	0.50
Regrowth Cycle 1	1277.7	0.63
Regrowth Cycle 2	1162.3	0.62

^aPore volume calculated from N₂ adsorption data at 77K at P/P₀ = 0.80

^bParent MOF refers to Al₄C₃-derived MIL-53(Al) precursor

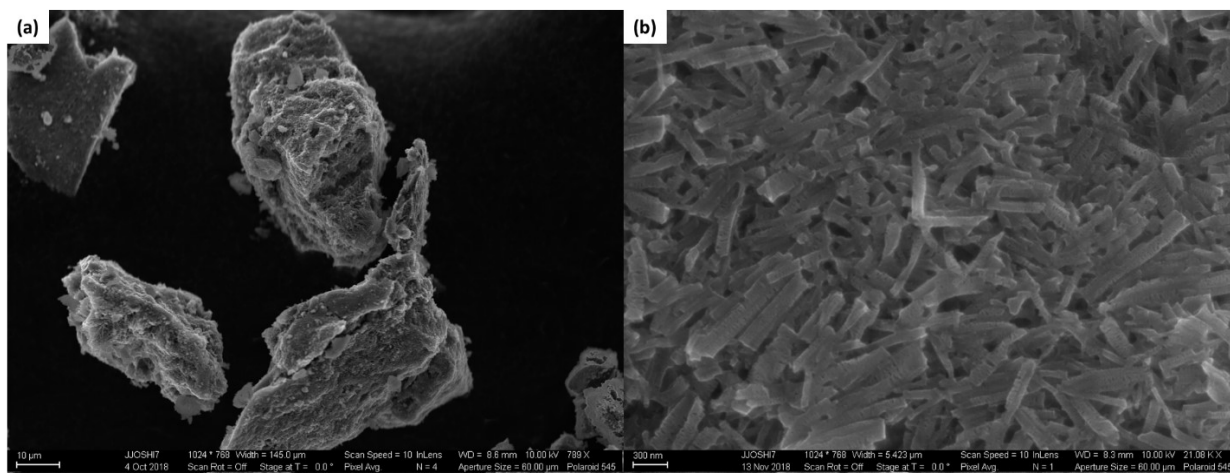


Figure S4. SEM images of MIL-53(Al)-derived oxide impregnated with iron oxide

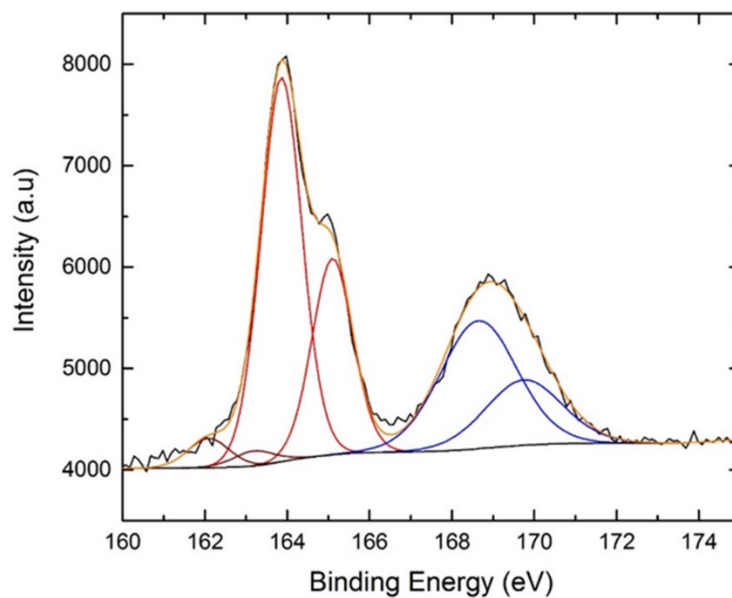


Figure S5. Fitted S_{2p} XPS data of iron oxide-impregnated MIL-53(Al)-oxide, following humid H₂S exposure

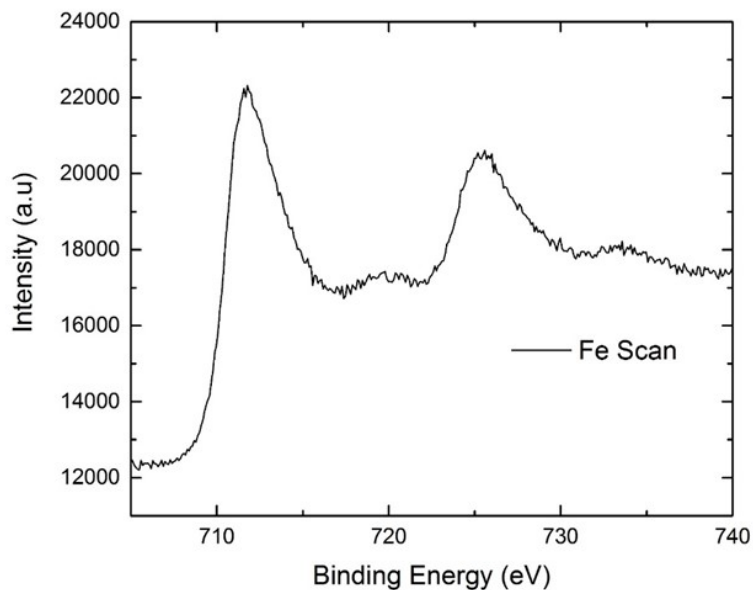


Figure S6. Fe 2p XPS spectrum of iron oxide-impregnated *MIL-53(Al)-oxide*, following humid H₂S exposure

Aluminum Carbide-Derived MIL-53(Al) - Pyrolysis Mass Loss

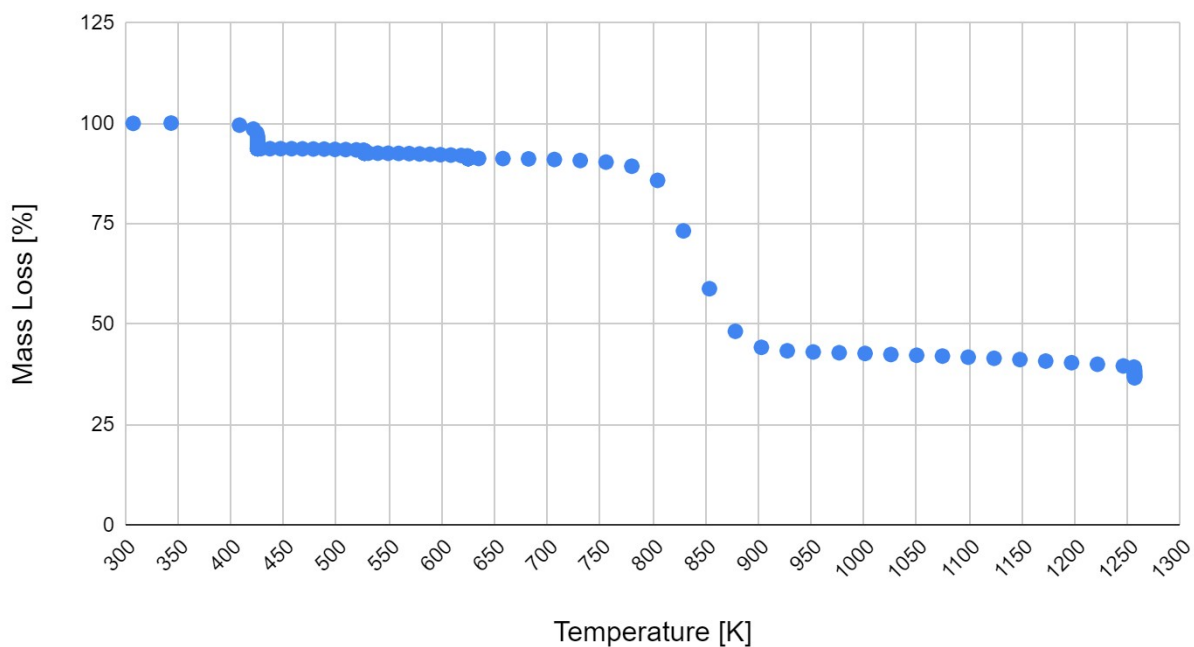


Figure S7. TGA mass loss curve of Al₄C₃-derived MIL-53(Al). Helium carrier gas used to create inert, non-oxygenated environment.

Table S2 – Reference Literature Hydrogen Sulfide Capacities to Related MOFs and Oxide Materials

MOF	Uptake Capacity [mmol S g⁻¹]	Reference	Notes
MIL-53(Al)	< 0.1	Hamon, L. <i>et al.</i> <i>J. Am. Chem. Soc.</i> 131 , 8775–8777 (2009)	Isothermal H ₂ S uptake experiments at 303K. Datapoint references at < 1kPa for comparison to work here
UiO-66(Zr)	< 0.5	Li, Z. <i>et al.</i> <i>Fluid Phase Equilib.</i> 427 , 259–267, (2016) Vaesen, S. <i>et al.</i> <i>Chem. Commun.</i> 49 , 10082–10084, (2013)	GCMC simulated H ₂ S uptake at 303K
MIL-125(Ti)	< 0.5	Costa, C. <i>et al.</i> <i>Materials.</i> 13 , 4725, (2020)	GCMC simulated H ₂ S uptake at 303K
Hematite Powder Adsorbent	0.8-0.9	Costa, C. <i>et al.</i> <i>Materials.</i> 13 , 4725, (2020)	Breakthrough at 150ppm H ₂ S, 298K

SI References

- (1) Moran, C. M.; Joshi, J. N.; Marti, R. M.; Hayes, S. E.; Walton, K. S. Structured Growth of Metal–Organic Framework MIL-53(Al) from Solid Aluminum Carbide Precursor. *J. Am. Chem. Soc.* **2018**, *140*, 9148–9153.
- (2) Moran, C. M.; Marti, R. M.; Hayes, S. E.; Walton, K. S. Synthesis and Characterization of Aluminum Carbide-Derived Carbon with Residual Aluminum-Based Nanoparticles. *Carbon N. Y.* **2017**, *114*, 482–495.
- (3) Walton, K. S.; Snurr, R. Q. Applicability of the BET Method for Determining Surface Areas of Microporous Metal–Organic Frameworks. *J. Am. Chem. Soc.* **2007**, *129*, 8552–8556.
- (4) Joshi, J. N.; Zhu, G.; Lee, J. J.; Carter, E. A.; Jones, C. W.; Lively, R. P.; Walton, K. S. Probing Metal–Organic Framework Design for Adsorptive Natural Gas Purification. *Langmuir* **2018**, *34*, 8443–8450.